Study on Applicability of Ground Settlement Prediction Method in Liquefaction Based on Energy Balance

S. Shimomura
College of Industrial Technology, Nihon University, Chiba, Japan

T. Adachi
College of Science and Technology, Nihon University, Tokyo, Japan

R. Asaeda
Tokyo-Kenchiku Structural Engineers, Tokyo, Japan

N. Sako
Nihon University Junior College, Chiba, Japan

SUMMARY
We proposed a new prediction method of ground settlement due to liquefaction based on the energy balance idea that had not hardly been studied. To discuss applicability of the proposed method, simulation analyses of the shaking table test results of the large scale shear box and of the actual seismic damage (1995 The Southern Hyogo prefecture earthquake and 2000 The Western Tottori prefecture earthquake) are conducted. From the simulation analysis results, it is confirmed that the proposed method can approximately predict the measurement value of the ground settlement whose value is from 0 to 50 cm.

Keywords: Liquefaction, Ground settlement, Energy

1. INTRODUCTION

The 2011 Off the Pacific Coast of Tohoku Earthquake caused extensive liquefaction in the city of Urayasu along the coast of Tokyo Bay. Reclaimed land accounts for about 75 percent of Urayasu City, and the earthquake caused liquefaction in almost all areas where liquefaction countermeasures had not been taken. Serious liquefaction damage consisted mainly of the settlement of small-scale houses, and the damage also included cave-ins in roads and exterior areas. Liquefaction has been observed in many of the recent major earthquakes such as the 1995 Hyogo-ken Nanbu Earthquake (Southern Hyogo Prefecture Earthquake) and the 2000 Tottori-ken Seibu Earthquake (Western Tottori Prefecture Earthquake). The degree of seismically induced damage varies widely depending on earthquake and ground conditions. It is difficult to evaluate the degree of earthquake-induced damage in terms of liquefaction alone, and ground surface settlement is a useful indicator of the degree of damage.

Ground surface settlement is reconsolidation settlement due to the dissipation of excess pore water pressure and can be obtained by mathematically integrating the vertical strains in soil layers in the direction of depth. If it is assumed that settlement occurs uniformly in the horizontal plane bounding semi-infinite ground, vertical strain is equivalent to volumetric strain. Undrained cyclic shear tests have shown that volumetric strains resulting from post-liquefaction reconsolidation are strongly correlated with the maximum shear strain during shaking (e.g., Lee and Albaisa, 1974). On the basis of the knowledge thus obtained, simple evaluation methods for liquefaction-induced ground surface settlement have been proposed (e.g., Tokimatsu *et al*., 1987).

It has been pointed out that excess pore water pressure, which is an indicator of the degree of liquefaction, is strongly correlated with the amount of energy calculated as the area of the shear stress–shear strain hysteresis loop. For superstructure, a seismic design method (Akiyama, 1985) based on the energy balance derived from Housner's (1956 & 1959) concept of energy input into a structure has been proposed. This method is based primarily on three items, namely, total energy input

into the structure of interest, energy distribution among layers and the energy absorption capacity of structural members in each layer. The degree of structural damage is evaluated in terms of the energy distributed among layers and the energy absorption capacity of structural members. This method is often used to design a seismically isolated structure that has a seismic isolation layer or elasto-plastic region with a large deformation capacity.

In order to evaluate the degree of earthquake-induced ground damage (excess pore water pressure, ground deformation) in a simple manner, the authors have proposed an energy balance-based method for rationally evaluating seismically induced ground behavior. The proposed method is an application of the energy balance-based seismic design method for superstructures. This paper briefly describes the proposed evaluation method and evaluates the usefulness of the method through simulation analyses of measured values of ground surface settlement.

2. PREDICTION METHOD FOR LIQUEFACTION DAMAGE LEVEL

2.1 ENERGY BALANCE OF GROUND

The seismic design method (Akiyama, 1985) based on the energy balance of the superstructure is based on the energy balance formula given by Eqn. 2.1;

$$\int_0^t \{\dot{x}\}^T [M]\{\ddot{x}\}dt + \int_0^t \{\dot{x}\}^T [C]\{\dot{x}\}dt + \int_0^t \{\dot{x}\}^T \{R\}dt = -\int_0^t \ddot{y}\{\dot{x}\}^T [M]\{i\}dt \tag{2.1}$$

where $[M]$ is the mass matrix; $[C]$, viscous damping coefficient matrix; $\{R\}$, restoring force vector; $\{\ddot{x}\}$, relative acceleration vector; $\{\dot{x}\}$, relative velocity vector; $\ddot{y}$, input ground acceleration; and $\{i\}=(1,1,1\cdots,1)^T$. The relative acceleration vector and the relative velocity vector are defined for the specified location of input ground acceleration. The first term on the left hand side is kinetic energy; the second term on the left hand side, energy consumed by damping; the third term on the left hand side, elasto-plastic strain energy; and the right hand side, input energy.

Eqn. 2.1 can be rewritten as

$$W_e + W_h + W_p = E \tag{2.2}$$

where W_e is elastic vibration energy (the sum of elastic strain energy and kinetic energy); W_h, energy consumed by damping; W_p, accumulated plastic strain energy; and E, input energy. Within the elastic range of ground, strains are very small, and elastic strain energy can be deemed to be zero. Elastic vibration energy W_e, therefore, may be deemed to be equal to kinetic energy W_k. Since ground is modeled as a unit soil column in this study, Eqn. 2.1 becomes an energy balance equation per unit area. Input ground acceleration is defined at the engineering base rock surface.

2.2 Outline of Prediction Method

Figure 2.1 shows the steps in the proposed evaluation method. Basically, the evaluation method consists of the three steps described below. For further details, please refer to previous reports (Shimomura *et al.*, 2010 & 2011).

Step 1: Calculate the energy contributing to damage to be input to ground.
Step 2: Calculate the energy contributing to damage distributed among layers.
Step 3: Evaluate the degree of liquefaction in each layer from the energy contributing to damage.

At Step 1, the energy input to the ground is evaluated first from the energy spectrum of the input earthquake motion by using the effective period that reflects the changes in the vibration period of ground due to the earthquake input. Then, by subtracting the viscous damping energy from the input

energy, the energy contributing to damage, E_D, is calculated. Since kinetic energy dissipates progressively, the energy contributing to damage corresponds to accumulated plastic strain energy.
At Step 2, shear stiffness, hysteresis damping factor, etc. in the case where the maximum value of the ratio of the effective shear strain obtained from equivalent linear analysis to the reference strain for

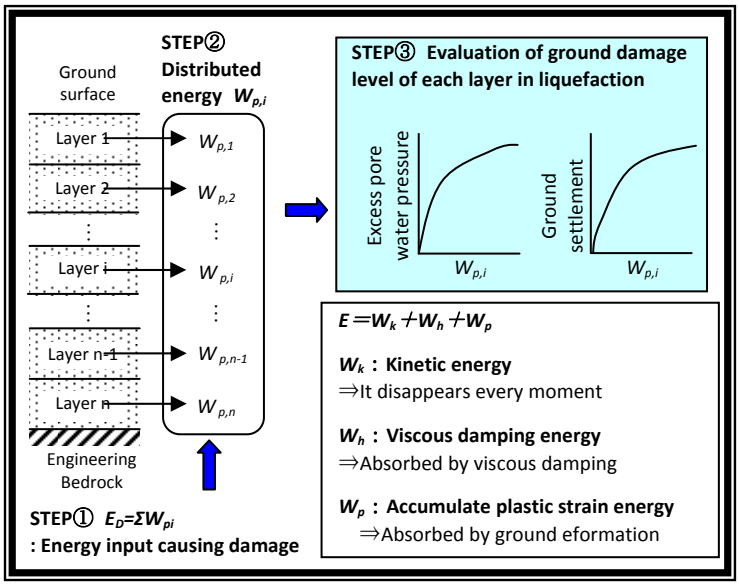

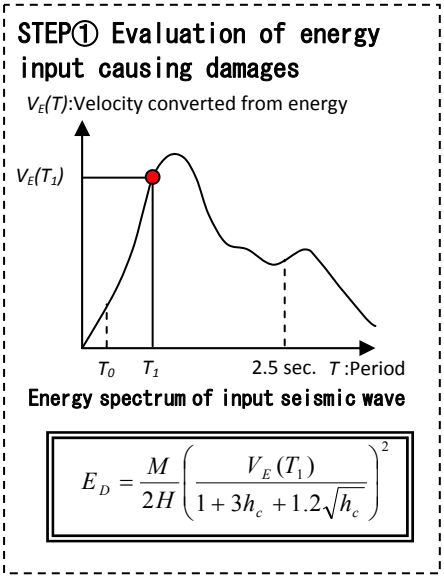

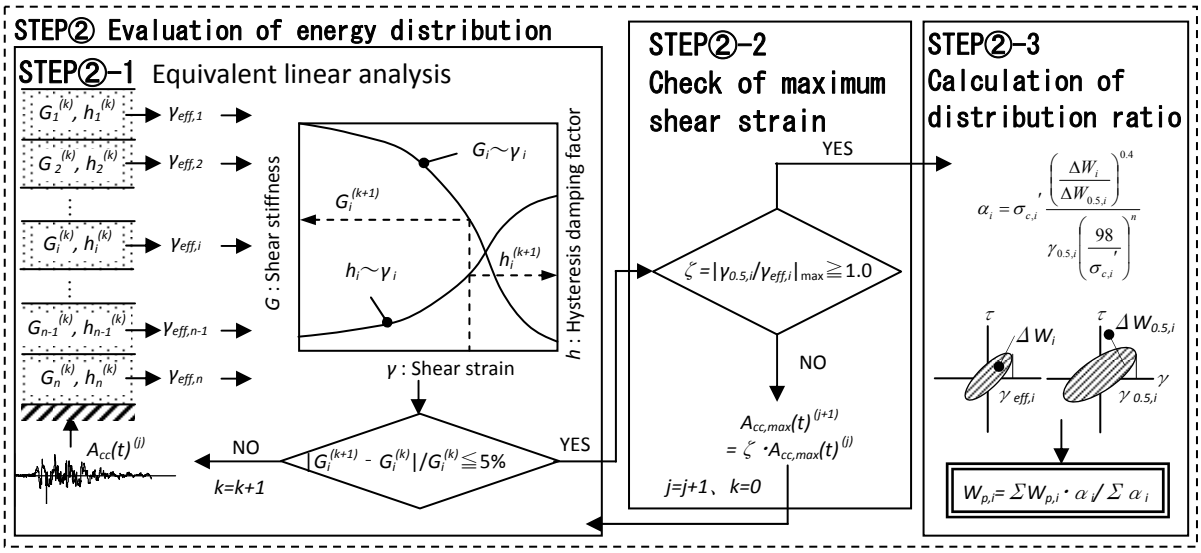

T_0 : Initial natural period of ground

T_1 : Effective period (= $\kappa \cdot T_0$)

$$\kappa = 13\sqrt{I(E)/\tau_{max}} + 1$$

$\overline{I(E)}$: Intensity of input motion (=M$\overline{V_E}^2$/2H)

τ_{max} : Shear strength of ground

$\overline{V_E}$: Average of VE from T_0 to 2.5sec.

$V_E(T_1)$: Velocity converted from energy at T_1

M : Mass

H : Layer thickness

h_c : Viscous damping factor

$A_{cc}(t)^{(j)}$: Acceleration time history of input motion at the time of the jth repetition calculation

$G_i^{(k)}$: Shear stiffness of layer i at the time of the kth repetition calculation (Initial shear stiffness at *k=0*)

$h_i^{(k)}$: Hysteresis damping factor of layer i at the time of the kth repetition calculation (Initial hysteresis damping factor at *k=0*)

$\gamma_{eff,i}$: Effective shear strain of layer i

$\gamma_{0.5,i}$: Reference shear strain of layer i

ΔW_i=Area of hysteresis loop at $\gamma_{eff,i}$

$\Delta W_{0.5,i}$= Area of hysteresis loop at $\gamma_{0.5,i}$

$\sigma_{c,i}'$: Initial effective confining stress of layer i

n : Constant (Sandy soil : 0.5, Cohesive soil : 0)

Figure 2.1. Evaluation procedure of liquefaction-induced ground damage based on energy balance

each layer is around one (1) are determined first (Step 2-1, 2-2). The areas of the hysteresis loops of the shear stress–shear strain curves for the effective shear strain and the reference strain (defined as the shear strain occurring when the initial shear stiffness has decreased by half) are calculated. On the basis of the ratio between them, the energy distribution ratio is calculated (Step 2-3). Then, the accumulated plastic strain energy $W_{p,i}$ for each layer is determined by multiplying the energy contributing to damage to be input to the ground determined at Step 1 by the distribution ratio.
At Step 3, if the purpose is to estimate the amount of settlement as an indicator of the degree of soil liquefaction, the relationship between the accumulated plastic strain energy and the volumetric strain is used (Figure 2.2 and Eqns. 2.3 to 2.5). Ground surface settlement is calculated by finding the amount of settlement from this relationship for each layer and integrating the amounts of settlement thus determined for the entire ground.

$$\varepsilon_v = aW_p^* / \sigma_c' \quad (\varepsilon_v < \varepsilon_{v,\max}) \qquad \varepsilon_v = \varepsilon_{v,\max} \quad (\varepsilon_v = \varepsilon_{v,\max}) \tag{2.3}$$

$$\varepsilon_{v,\max} = 0.003 R_{15}^{-1.4} \tag{2.4}$$

$$a = 0.010 R_{15}^{-3.1} \tag{2.5}$$

where a is the reconsolidation gradient (the gradient of the line shown in Figure 2.2); $\varepsilon_{v,max}$, maximum volumetric strain (volumetric strain levelling off in Figure. 2.2); and R_{15}, liquefaction resistance (defined, in an undrained cyclic shear test, by the shear stress ratio at which the full amplitude of shear strain in 15 loading cycles reaches 7.5%).

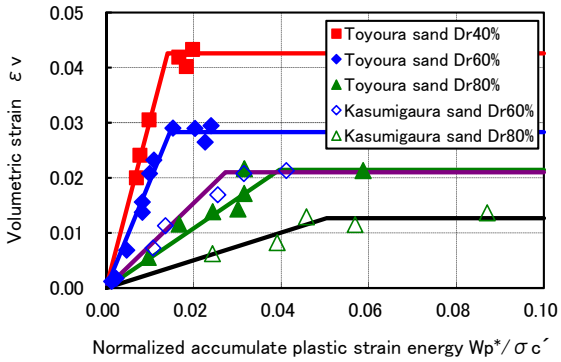

Figure 2.2. Relationship between volumetric strain and Normalized accumulate plastic strain energy

3. SIMULATION ANALYSIS

In this section, the applicability of the proposed evaluation method through a simulation analysis using measured values of ground surface settlement. The measured values used were obtained from shaking table tests conducted by using a large-scale shear box, at Kobe Port Island (hereinafter referred to as "Kobe PI") during a real earthquake (1995 Hyogo-ken Nanbu Earthquake) and at the Takenouchi Industrial Complex (hereinafter referred to as "Takenouchi") in the city of Sakaiminato, Tottori Prefecture, during the 2000 Tottori-ken Seibu Earthquake.

3.1 Shaking Table Test Using Large-scale Shear Box

3.1.1 Test and analysis conditions

The purpose of the test (Tamura *et al.*, 1999 & 2002) was to investigate the seismic behavior of reinforced concrete piles and steel pipe piles in liquefiable soil. The piles were installed in advance in a large-scale shear box (12.0 m wide [in the direction of excitation], 3.5 m deep and 6.0 m high). The test was conducted by using a large shaking table (15.0 m × 14.5 m) at the National Research Institute

for Earth Science and Disaster Prevention.

Table 3.1 shows the test conditions and test results used in the analysis. In the table, the test conditions and results for reinforced concrete piles are shown in Ground Condition Category 1, and the test conditions and results for steel pipe piles in Ground Condition Category 2. The soil used in the test was prepared by the water sedimentation method by using river sand (particle density 2.718 g/cm^3, maximum void ratio 0.961, minimum void ratio 0.570) in a slightly moist (air-dried) condition. The water level was at ground level. Ground Condition Category 2 has a layer consisting of bags of gravel (layer thickness about 150 cm, *Vs* = 228 m/s) at the bottom. In each test, the test ground was used repeatedly. The relative density of the ground used for the testing, therefore, was calculated, by using the initial density (assumed to be 52% for both ground condition categories) as a reference density, from the amount of change in ground level measured after each test. The changes in ground level were calculated on the assumption that vertical strain occurred uniformly in only the saturated sand layers.

Table 3.1. Experimental condition and result

Ground condition	Case No.	Maximum input Accleration (m/s^2)	Ground thickness (cm)	Measurement ground settlement (cm)	Shear velocity of sand layer Vs(m/s)	Relative density Dr(%)
1	1−1	0.3	590	2	106	52
	1−2	0.3	589	2	103	53
	1−3	0.45	579	2	97	60
	1−4	3.1	579	10	105	60
2	2−1	0.1	558	0	82	52
	2−2	0.3	558	0	82	52
	2−3	0.6	558	7	82	52
	2−4	0.9	545	8	77	63
	2−5	0.9	552	10	78	57
	2−6	0.6	541	9	73	66

Figure 3.1 shows the relationship between the liquefaction resistance R_{15} obtained from the results of undrained cyclic shear tests conducted by using a hollow torsional shear apparatus and the relative density *Dr*. Relative density in the large-scale shear box tests varied among test cases. The relationship, therefore, between normalized accumulated plastic strain energy and volumetric strain was determined by estimating liquefaction resistance from relative density from Eqn. 3.1 approximating Figure 3.1 and substituting the value thus obtained in Eqns. 2.3 to 2.5.

$$R_{15} = 0.002D_r + 0.07 \tag{3.1}$$

where D_r is the relative density (%).

Figure 3.2 shows the acceleration time history and energy spectrum of the input seismic wave. The input seismic wave used was obtained by adjusting the maximum acceleration and duration of the artificial seismic wave RINKAI-92 (maximum acceleration 3.1 m/s^2). Excitation is unidirectional.

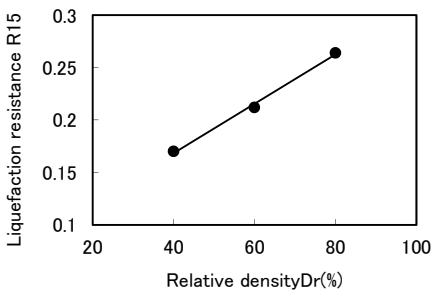

Figure 3.1. Relationship between relative density and liquefaction

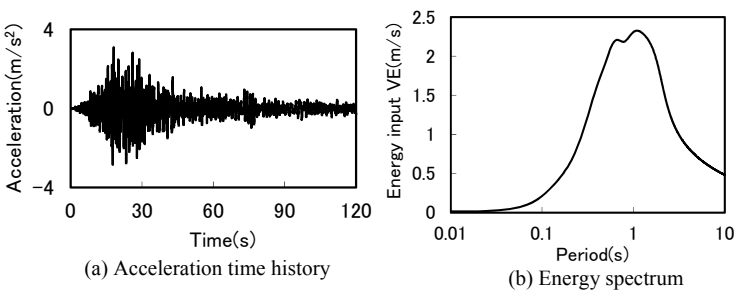

(a) Acceleration time history

(b) Energy spectrum

Figure3.2. Input seismic wave

Table 3.2 shows an example of a ground model used for the purpose of analysis. In the analysis, the ground was more or less equally divided into seven layers. The reference strain under the initial effective confining stress of 98 kPa is 1.13×10^{-3}, and the maximum damping factor is 0.28. The reference strain was determined by (1) calculating the initial effective confining stress by assuming a coefficient of earth pressure at rest of $K_0 = 0.5$ and (2) assuming that the reference strain is proportional to the 0.5th power of the initial effective confining stress. The reference strain and the maximum damping factor for the gravel layer under the Category 2 ground conditions were determined with reference to literature (Architectural Institute of Japan, 2006). The viscous damping factor was assumed to be zero, and a hyperbolic model was used for the G/G_0–γ and h–γ relationships.

Table 3.2. Example of ground model

Case No.	Relative density (%)	Soil	Thickness of each layer (m)	Initial shear stiffness (MPa)	Reference strain ($\times 10^{-4}$)	Maximum hysteresis damping factor
1−1	52	Sand	0.84	9	1.9	0.28
				15	3.3	
				19	4.2	
				23	5.0	
				26	5.7	
				29	6.3	
				31	6.8	
2−1	52	Sand	0.81	6	1.8	0.28
				10	3.2	
				13	4.1	
				16	4.8	
				18	5.5	
	−	Gravel	0.77	106	4.0	0.21
				116	4.4	

3.1.2 Analysis results

Figure 3.3 shows examples of the vertical distributions of the initial shear stiffness, the accumulated plastic strain energy distribution ratio and volumetric strain. As shown, the energy distribution ratios of the sand layers increase with depth although density is uniform. This corresponds to the fact that the energy distribution ratio is proportional to the initial effective confining stress. The results for Ground Condition Category 2 show that the energy distribution ratio of the gravel layer is smaller than that of any of the overlying sand layers although the initial effective confining stress is large. This corresponds to the fact that energy concentration occurs because the shear stiffness of the sand layers is by far lower than that of the gravel layer and, therefore, the degree of nonlinearity increases significantly. Volumetric strain tends to increase as the input acceleration increases and as relative density decreases. In Case 1-4 and Case 2-4, volumetric strain reached the maximum value in all sand layers. In the cases where volumetric strain did not reach the maximum value, however, an opposite tendency (normalized accumulated plastic strain energy decreases and volumetric strain decreases as the initial effective confining stress increases) was observed (Figure. 2.2). The initial effective confining stress tends to be larger in deeper layers, and both normalized accumulated plastic strain energy and volumetric strain can decrease even if the energy distribution ratio is large. This tendency can be seen in the cases in which volumetric strain did not reach the maximum value.

Figure 3.4 shows the relationship between the measured values and predicted values of settlement. As shown, predicted settlements (about 0 to 18 cm) tend to be somewhat larger than measured settlements (about 0 to 10 cm), but the proposed evaluation method gives values that show a relatively low degree of variability and fairly good agreement with the measured values over a wide range from a low level at which settlement does not occur to a high level at which the maximum volumetric strain is reached in practically every part of the ground.

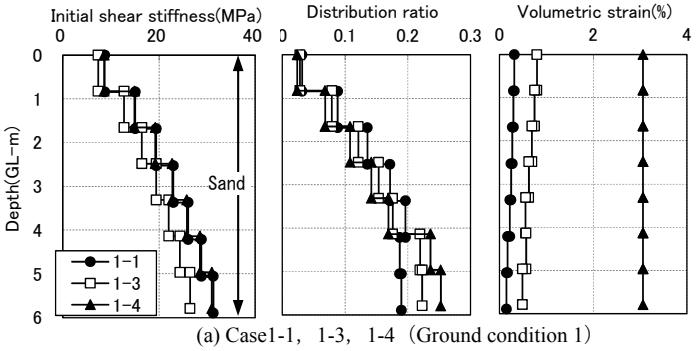

(a) Case1-1, 1-3, 1-4 (Ground condition 1)

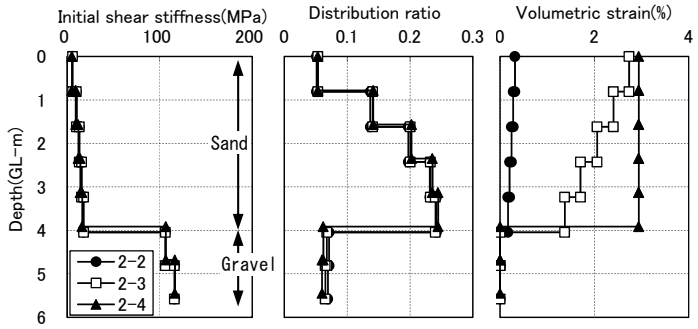

(b) Case2-2, 2-3, 2-4 (Ground condition 2)

Figure 3.3. Distribution of initial shear stiffness, energy distribution ratio and volumetric strain

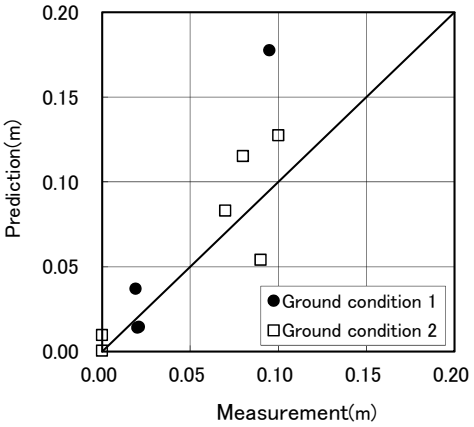

Figure 3.4. Relationship between measured settlement and predicted settlement

3.2 Actual Damage Due to Earthquake

3.2.1 Analysis conditions

Table 3.3 shows the ground model used for the analysis of Kobe Port Island (Kobe PI). The ground model was designed, by referring to literature (Kobe City Report, 1995 & Yoshida, 1995), to cover depths down to GL−83 m. The ground was divided into layers having a thickness of about 2.5 m. Settlement calculation was performed only for reclaimed layers, and their liquefaction resistance was assumed to be 0.15 to 0.22 (Hatanaka, 1997). The measured values of settlement at Kobe PI except the soil improvement zones were about 30 to 60 cm (Kobe City Report, 1995).

Table 3.4 shows the model used for the analysis of Takenouchi. The Takenouchi ground model was designed, by referring to literature (Mori & Kazuni, 2006), to cover depths down to GL−67 m. The ground was divided into layers having a thickness of about 3 m. The reference strain and the maximum damping factor were determined by referring to previously reported data (Architectural Institute of Japan, 2006). Because the occurrence of liquefaction was observed in the silt layers at the site (Mori & Kazuni, 2006), settlement calculation was performed for the layers above GL−31 m including the silt layers. The liquefaction resistance of the sand layers was determined, by using the N-value (SPT blow count) and referring to literature (Tokimatsu *et al.,* 1983), as liquefaction resistance under the laboratory conditions. In view of the fact that the silt layers with a high fine content had liquefied, it was judged that the plasticity of the fines contained in the sand layers was low and therefore their influence on liquefaction resistance was small. No correction was made, therefore, of the N-values. The liquefaction resistance of the silt layers was assumed to be 0.08 to 0.25 (Yoshimoto *et al.,* 2002, Sako *et al.,* 2001 & Numata *et al.,* 2002). The measured values of settlement at Takenouchi ranged from about 20 to 40 cm (Tsukamoto & Ishihara, 2010). At both sites, the reference strains for the sand layers and gravel layers were varied in proportion to the 0.5th power of the initial effective confining stress obtained by assuming a coefficient of earth pressure at rest of K_0 = 0.5.

Figures 3.5 and 3.6 show the acceleration time history and energy spectrum of the seismic wave given at the bottom (assumed to act as the engineering base rock) of the ground model. For the Kobe PI

results, the GL−83 m records obtained at Kobe City Development Bureau were used. For the Takenouchi results, the ground level observation records obtained at the Mihonoseki monitoring station as part of the Digital Strong-Motion Seismograph Network of the National Research Institute for Earth Science and Disaster Prevention were used. The Mihonoseki monitoring station is close to Takenouchi, and the ground there consists mainly of rock having a shear wave velocity of 500 m/s or more at depths of 4 m or more. It may be thought, therefore, that seismic waves observed at ground level are practically free from the influence of the surface layer of the ground. This is why it was thought that the seismic waves observed at ground level are suitable for use as seismic waves to be input to the engineering base rock. For both seismic waves, the energy spectra were obtained by adding together the input energy of the two components in the NS and EW directions. For both ground models, the viscous damping factor was assumed to be zero, and a hyperbolic model was used for the G/G_0–γ and h–γ relationships.

Table 3.3. Example of ground model (Kobe PI)

Bottom depth (m)	Soil	R15		Initial shear stiffness (MPa)	Reference strain ($\times 10^{-4}$)	Maximum Hysteresis damping factor
		Min.	Max.			
3	Reclaimed layer (Gravel)	0.15	0.22	53	1.6	0.23
6				64	2.4	0.23
8				74	2.8	0.23
11				83	3.1	0.23
14				91	3.4	0.23
16				98	3.7	0.23
19				104	4.0	0.23
22	Clay	–		50	14.0	0.23
24				52	14.0	0.23
27				53	14.0	0.23
30	Sand			109	7.2	0.23
32				114	7.5	0.23
35				119	7.8	0.23
37				123	8.1	0.23
40	Sand			168	8.4	0.23
42				174	8.7	0.23
45				179	9.0	0.23
47				185	9.3	0.23
50				190	9.5	0.23
53				226	9.8	0.23
56				232	10.1	0.23
58				238	10.3	0.23
61				244	10.6	0.23
63	Clay			159	19	0.17
66				162	19	0.17
68				165	19	0.17
71				168	19	0.17
73				171	19	0.17
76				174	19	0.17
78				176	19	0.17
81				179	19	0.17
83				182	19	0.17

Table 3.4. Example of ground model (Takenouchi)

Bottom depth (m)	Soil	N−value	R15		Initial shear stiffness (MPa)	Reference strain ($\times 10^{-4}$)	Maximum Hysteresis damping factor
			Min.	Max.			
3	Sandy silt	2	0.08	0.25	30	18.0	0.17
6	Silty sand	2	0.10		14	4.0	0.21
9		2	0.10		17	4.9	0.21
11	Sand	15	0.29		63	5.5	0.21
13	Sandy silt	2	0.08	0.25	26	18.0	0.17
16	Silty sand	7	0.19		38	6.5	0.21
19		6	0.18		41	7.0	0.21
22	Sandy silt	2	0.08	0.25	24	18.0	0.17
25		2	0.08	0.25	26	18.0	0.17
28		2	0.08	0.25	27	18.0	0.17
31		2	0.08	0.25	28	18.0	0.17
34	Volcanic sand	12	–		62	9.2	0.21
37		9			65	9.6	0.21
40		16			68	10.0	0.21
43		14			71	10.4	0.21
46		15			73	10.8	0.21
49	Sandy silt	7			62	18.0	0.17
52		7			63	18.0	0.17
55		7			65	18.0	0.17
58		7			66	18.0	0.17
61	Silt	23			92	18.0	0.17
64	Silty sand	15			97	12.6	0.21
67		35			99	12.9	0.21

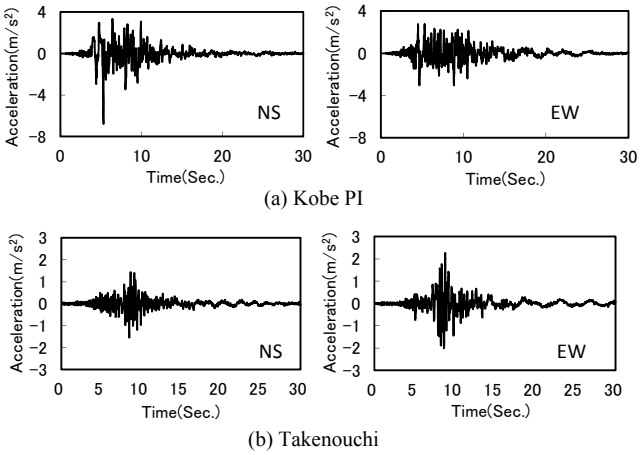

(a) Kobe PI

(b) Takenouchi

Figure 3.5. Acceleration time history of input seismic wave

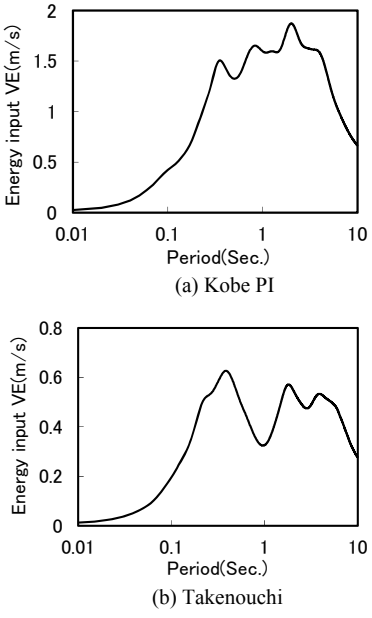

(a) Kobe PI

(b) Takenouchi

Figure 3.6. Energy spectrum of input seismic wave

3.2.2 Analytical results

Figure 3.7 shows the vertical distributions of the initial shear stiffness, the accumulated plastic strain energy distribution ratio and volumetric strain. In connection with the depths considered by assuming a certain range of volumetric strain, the range of volumetric strain is shown as a hatched area. The large-scale shear box simulation analysis results indicate that energy tends to be concentrated in layers whose initial shear stiffness is low. The real-earthquake simulation results, however, do not necessarily show such tendencies. This is due in part to the fact that the large-scale shear box deals with sand and gravel, which have relatively similar shear stiffness decrease tendencies, while the real ground consists of alternating layers of sand and clay, which differ significantly in shear stiffness decrease tendency. This means that because cohesive soil is more viscous than sandy soil, the cohesive soil layers show a higher degree of nonlinearity than the sandy soil layers, indicating a tendency to be less prone to energy concentration. Because of dependence, however, on the initial shear stiffness and interlayer differences in reference strain, this tendency varies depending on the ground structure. Volumetric strain reached the maximum value in all reclaimed layers at Kobe PI, while it did not reach the maximum value in all layers at Takenouchi. Estimated amounts of settlement are 40 to 68 cm at Kobe PI and 24 to 54 cm at Takenouchi.

Figure 3.8 shows the relationship between measured values and predicted values of settlement. The amount of settlement is shown in the form of the average of the maximum and minimum values partly because settlement at each site was measured at a number of locations and partly because predicted amounts of settlement were obtained from a certain range of liquefaction resistance. Figure 3.8 also shows the large-scale shear box simulation results shown in Figure 3.4. As Figure 3.8 indicates, the proposed method makes it possible to roughly predict a wide range of settlements from zero settlement to about 50 cm and a wide range of damage from light damage causing only less-than-maximum volumetric strains to extensive damage causing volumetric strain to reach the maximum value in all layers.

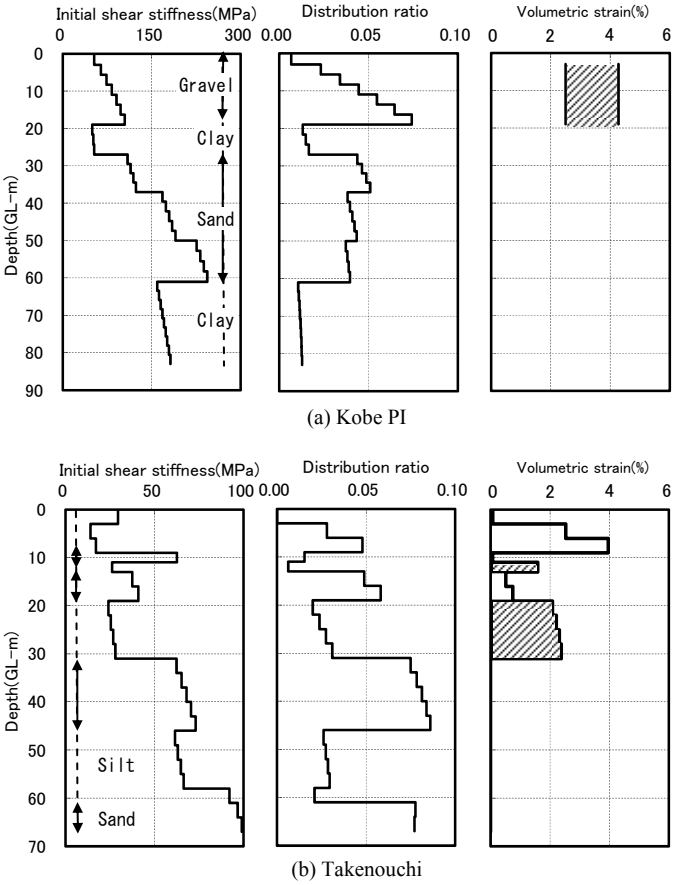

Figure 3.7. Distribution of initial shear stiffness, energy distribution ratio and volumetric strain

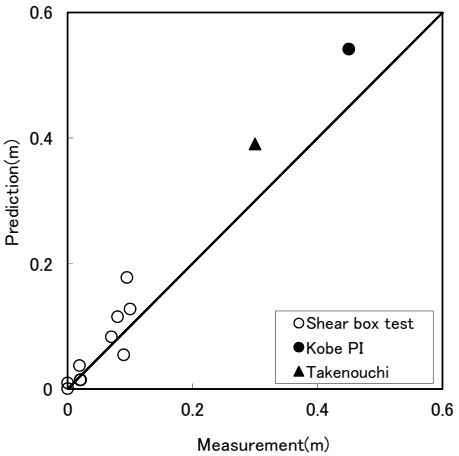

Figure 3.8. Relationship between measured settlement and predicted settlement

4. Conclusion

The purpose of this study is to develop an energy balance-based evaluation method for predicting the seismic behavior of ground. Given an energy spectrum showing external force, the proposed method is capable of predicting not only the properties of ground commonly used in seismic response analysis but also the amount of ground settlement due to liquefaction. This paper has evaluated the applicability of the proposed evaluation method through simulation analyses using ground settlement measurement results obtained from shaking table tests using a large-scale shear box and measured values of earthquake-induced settlement. The study results thus obtained indicate that the proposed evaluation method is applicable because differences in ground structure (initial shear stiffness of ground and type of ground) can be reflected in the energy given to each layer as an external force and because ground settlement estimates obtained by the proposed evaluation method show fairly good agreement with a wide range of measured values of settlement.

REFERENCES

Akiyama, H. (1985). Earthquake-Resistant Limit-State Design for Buildings: University of Tokyo

Architectural Institute of Japan (2006). Seismic Response Analysis and Design of Buildings Considering Dynamic Soil-Structure Interaction, 56, in Japanese

Hatanaka, M., *et al.* (1997). Liquefaction characteristics of a gravelly fill liquefied during the 1995 Hyogo-ken Nanbu earthquake. *Soils and Foundations*. **Vol.37. No.3**: JGS, 107-115

Housner, G.W. (1959). Behaviour of structures during earthquakes. *Journal of the Engineering Mechanics Division.* **Vol.85. No.EM4**: Proc. ASCE, 109-129

Housner, G.W. (1956). Limit design of structures to resist earthquakes. *Proc. of 1st. WCEE*, 1-13

Kobe City Report (1995). Investigation of ground deformation of reclaimed ground due to Hyogo-ken Nanbu earthquake, Port Island, Rokko Island, in Japanese

Lee, K. L. and Albaisa, A. (1974). Earthquake induced settlements in saturated sands. *Journal of the Geotechnical Engineering Division*. **Vol.100. No.GT4**: Proc. ASCE, 387-406

Mori, S. and Kazuni, S. (2006). Seismic Response of Severely Liquefied Grounds on Reclaimed Lands in Sakai-minato City. *The 12th Japan Earthquake Engineering Symposium*, 538-541, in Japanese

Numata,A., *et al.* (2002). Liquefaction resistance on Takenouchi silt. *Proceedings of Annual Conference of The Japan Society of Civilengineers*. **Vol.57**, 1153-1154, in Japanese

Sako, N., *et al.* (2001). Liquefaction strength of sand erupted during Tottori-ken Seibu Earthquake, *Proceedings of the 36th Japan National Conference on Geotechnical Engineering*, 395-396, in Japanese

Shimomura, S., *et al.* (2010). Study on evaluation of ground motion in earthquake based on energy balance –Evaluation of level of damage and energy input in saturated sandy ground-. *Journal of structural and construction engineering*. **Vol.650**: Architectural Institute of Japan, 807-815, in Japanese

Shimomura, S., *et al.* (2011). Evaluation of viscous damping energy and energy distribution in multi-layered ground -Study on evaluation of ground motion in earthquake based on energy balance Part 2-. *Journal of structural and construction engineering*. **Vol.661**: Architectural Institute of Japan, 553-562, in Japanese

Tamura, S., *et al.* (1999). Shaking table test of a reinforced concrete pile foundation on liquefied sand using a large-scale laminar shear box. *Technical note of the National Research Institute for Earth Science and Disaster Prevention*. **Vol.190**, 1-109, in Japanese

Tamura, S., *et al.* (2002). Shaking table test of a steel pile foundation on liquefied sand using a large scale laminar shear box, *Technical note of the National Research Institute for Earth Science and Disaster Prevention*. **Vol.227**, 1-64, in Japanese

Tokimatsu, K. and Yoshimi, Y. (1983). Empirical correlation of soil liquefaction based on SPT N-value and fines content, *Soils and Foundations*. **Vol.23. No.4.** JGS, 56-74

Tokimatsu, K. and Seed, H. B. (1987). Evaluation of settlements in sands due to earthquake shaking. *Journal of the Geotechnical Engineering Division*. **Vol.113. No.GT8**: ASCE, 861-878

Tsukamoto, Y. and Ishihara, K. (2010). Analysis on settlement of soil deposits following liquefaction during earthquakes. *Soils and Foundations*. **Vol.50. No.3**: JGS, 399-411

Yoshida, N. (1995). Earthquake response analysis at Port Island during the 1995 Hyogoken-nanbu Earthquake, *Tsuchi-to-Kiso*. **Vol.43. No.10**: JGS, 49-54, in Japanese

Yoshimoto, N., et al. (2002). Characteristics of the fines soils liquefied in The Tottori Ken Seibu Earthquake. *Journal of Japan Society of Civil Engineers*. **No.722/Ⅲ-61**, 85-96, in Japanese